

Comparative Study on the Effectiveness of UPFC and TCSC for Increasing Power Transfer Capability Applied to Non-linear Load Models

S. Ali Al-Mawsawi

Department of Electrical and Electronics Engineering, College of engineering, University of Bahrain,
P. O. Box 32038, Isa Town, Kingdom of Bahrain
Corresponding author, e-mail: aalmossawi@uob.edu.bh

Abstract

In recent years, studies have been investigated the effectiveness of UPFC and TCSC in increasing power transfer capability. However, the effectiveness of these FACTS devices in increasing power transfer capability when the load is non-linear has not been established in a comparative study yet. This paper will explore the steady-state performance of the UPFC and TCSC as impedance compensation models. The effectiveness of both FACTS devices are investigated when they are installed in multi-machine systems with different non-linear load models. Simulation results demonstrate that, upon installing UPFC, more active and reactive powers are received at the sending end bus for different types of non-linear load models. In addition, both active and reactive powers are more sensitive in changing the modulation index of the converters. Furthermore, both the active and reactive powers are less sensitive to the non-linearity of the load model type. However, active and reactive powers in case of installing TCSC are only sensitive in changing the firing angle (α) when it is between 90° to 110° . Therefore, results from this study clearly encourage the effectiveness of UPFC in comparison to TSCS in terms of increasing power transfer capability applied to non-linear load models.

Keywords: UPFC, TCSC, PWM, Firing Angle, Non-Linear Load Models

Copyright © 2017 Institute of Advanced Engineering and Science. All rights reserved.

1. Introduction

In the late 1980s, the Electric Power Research Institute (EPRI) formulated the vision of the Flexible AC Transmission Systems (FACTS) in which various power-electronics based controllers regulate power flow and transmission voltage and mitigate dynamic disturbances. Generally, the main objectives of FACTS are to increase the useable transmission capacity of lines and control power flow over designated transmission routes [1]. Since then, many FACTS devices have been introduced such as Static Var Compensator (SVC), Thyristor-Controlled Series Capacitor (TCSC), Thyristor-Controlled Phase Shifter (TCPS), Static Synchronous Compensator (STATCOM), Static Synchronous Series Compensator (SSSC), Unified Power Flow Controller (UPFC), and the Interline Power Flow Controller (IPFC) [2-10]. The installation of the Unified Power Flow controller (UPFC) and Thyristor- Controlled Series Capacitor (TCSC) in power systems has recently come under intensive investigation into its modeling and various control functions, including damping control for multi-machine power systems^[11]. Work has been done to model the UPFC and TCSC into multi-machine power systems in a steady-state mode of operation for studying power flow control [12, 13]. However, most of the studies were based on the assumption that the load is linear of infinite bus [11-16]; which is practically untrue.

This paper discusses with the mathematical modeling and analysis of a TCSC and a Pulse-Width-Modulation (PWM) based UPFC operating as impedance compensation implemented on a multi-machine power systems connected to a non-linear load model. The steady-state performance simulation results of the system are presented and compared for different non-linear load model.

2. Steady-State Model of Thyristor-Controlled Series Capacitor (TCSC)

TCSC is one of the most important and best known FACTS devices, which has been in use for many years to increase the power transfer as well as to enhance system stability. The main circuit of a TCSC is shown in Figure 1. Figure 1 illustrates a TCSC which consists of a series compensating capacitor (C) shunted by a thyristor controlled reactor (TCR).

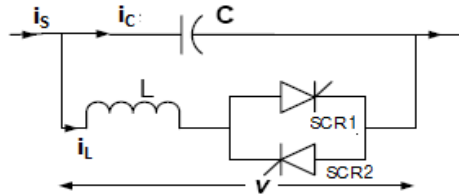


Figure 1. Configuration of a TCSC

The firing angles (α) of the thyristors are controlled to adjust the TCSC reactance in accordance with a system control algorithm, normally in response to some system parameter variations. According to the variation of the thyristor firing angle or conduction angle, this process can be modeled as a fast switch between corresponding reactance's offered to the power system. Series capacitive compensation is an old and economic technique to increase the power transfer capability of a long transmission line. Since 1950, fixed series capacitors were installed in long alternating – current transmission lines to cancel a part of the inherent inductive reactance. If 70% line inductive reactance is cancelled, then line is said to have 70% of series compensation and degree of series compensation (K) is 70%. However, 100% compensation will raise a problem of series resonance in the system. In such case, if the TCR is a variable inductive reactor ($X_L(\alpha)$) tuned at firing angle, the variation of X_L with respect to α can be given as [17]:

$$X_L(\alpha) = X_L \frac{\pi}{(\pi - 2\alpha - \sin 2\alpha)} \quad (1)$$

$$X_C = -\frac{1}{2\pi f C} \quad (2)$$

The effective TCSC reactance X_{TCSC} with respect to alpha (α) can be given as:

$$X_{TCSC}(\alpha) = -X_C + C_1(2(\pi - \alpha) + \sin(2(\pi - \alpha))) - C_2 \cos^2(\pi - \alpha)(w \tan(w(\pi - \alpha)) - \tan(\pi - \alpha)) \quad (3)$$

Where;

$$C_1 = \frac{X_C + X_L}{\pi} \quad (4)$$

$$C_2 = 4 \frac{X_{LC}^2}{\pi X_L} \quad (5)$$

$$X_{LC} = \frac{X_C X_L}{X_C - X_L} \quad (6)$$

$$w = \sqrt{\frac{X_C}{X_L}} \quad (7)$$

Figure 2 represents the reactance characteristics curve of a TCSC device. It shows the operation in both capacitive and inductive regions through variation of firing angle (α). The operation of TCSC can be summarized as shown in Table 1.

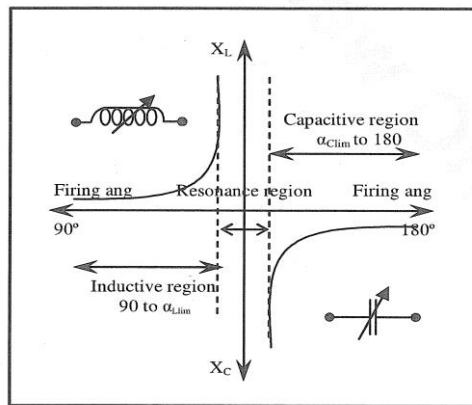


Figure 2. Reactance characteristics curve of a TCSC device

Table 1. Operation of TCSC device

Range of firing angle (α)	Region
$90^\circ \leq \alpha \leq \alpha_{Lim}$	Inductive region
$\alpha_{Clim} \leq \alpha \leq 180^\circ$	Capacitive region
$\alpha_{Lim} \leq \alpha \leq \alpha_{Clim}$	Resonance region

3. Steady-State Model of Unified Power Flow Controller (UPFC)

Figure 3, which presents a construction of the unified power flow controller (UPFC), depicts that UPFC is composed of a shunt compensation block and a series compensation block connected through a common dc link capacitor. The main purpose of the shunt compensation block is to provide a real power to a series compensation block. Furthermore, it is capable to control the reactive power in the transmission line. In the other hand, the series compensation block is capable of controlling the real power flow in the transmission line through three types of compensation (voltage regulation, series impedance compensation and phase shift compensation). These types of compensation can be achieved by controlling the magnitude and phase angle of the injected series voltage.

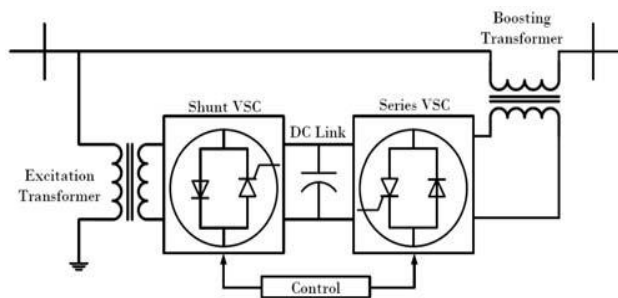


Figure 3. Unified Power Flow Controller (UPFC) Construction

One study deduced that UPFC can be modeled as seen in Figure 4 [18]. As observed, both compensation blocks are replaced by two independent voltage sources. Where, the magnitude and the phase angle of both sources can be controlled. The shunt and the series transformers are replaced by equivalent leakage reactance. It is assumed that, the two voltage sources are dependent of each other and the real power exchange by them should be satisfied:

$$P_{Et} + P_{Bt} = 0 \tag{8}$$

Therefore, in order to satisfied equation (8), it is also assumed that, the equivalent leakage reactances of both transformers are neglected and the UPFC is a loss less system.

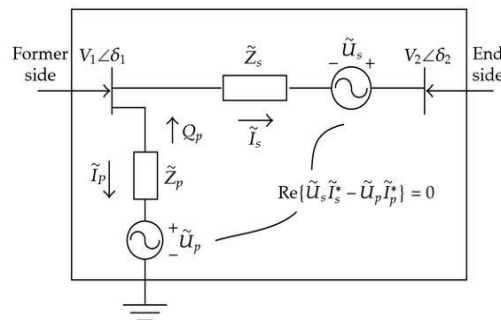


Figure 4. UPFC Equivalent Circuit

Most of the previous UPFC load flow studies have been presented an innovative approach [18, 19], where the equivalent bus representation in Figure 4 was used. In this representation, the UPFC is intended for simultaneous control where it will control the real power flow through the transmission line, regulate the receiving end voltage and control reactive power injection to the sending end bus. Consequently, the sending bus is set to a PQ - load bus and the receiving end bus is set to a PV generator bus. By the assumption that the UPFC is a lossless system and from equation (8), one can draw inference that the real power for the load bus and for the generator bus are equal and are set to the desired power flow in the transmission line that the UPFC should control. Therefore, the UPFC is cable to control simultaneously or separately both the real and reactive powers flow in the transmission line. Thus, Figure 5 represents different control schemes that can be used for simultaneous decoupled control model.

A scheme presented in Figure 5(a) can be used for controlling the real power flow through the line and regulating the voltage at the sending end bus. The scheme shown in Figure 5(b) is used when it is required to achieve double parameter control. In this case, both buses are represented as PQ buses. Equation (8) is used to set the real power and the injected reactive power by the shunt compensation block to be zero ($Q_{Et} = 0$). Thus, both real and reactive powers flow in the transmission line can be controlled. The voltage regulation and the real power flow control can be achieved at both buses by using the scheme presented in Figure 5(c).

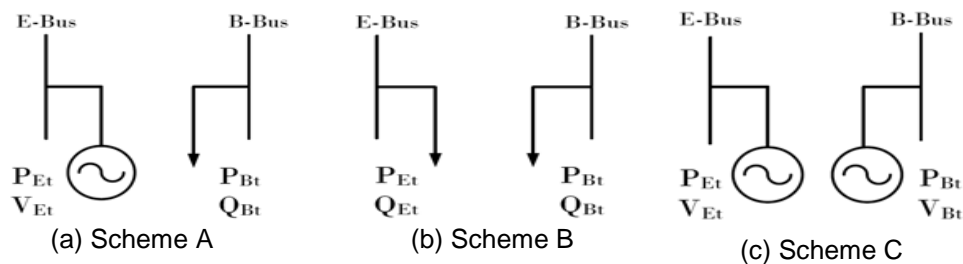


Figure 5. UPFC Equivalent Bus Representation

If the control strategy for the UPFC is decided, then it is replaced by one of the schemes bus representation and the steady-state load flow in the transmission line can be solved. Furthermore, the control parameters of the UPFC can be found by obtaining all the state variables of the network system with the decoupled representation of the UPFC. The following equations have been used to model the steady-state power flow injections for the UPFC.

$$P_{Etc} = \frac{V_{Et}V_E}{X_E} \sin(\delta_{Et} - \delta_E) + \frac{V_{Et}V_{Bt}}{X_B} \sin(\delta_{Et} - \delta_{Bt}) - \frac{V_{Et}V_B}{X_B} \sin(\delta_{Et} - \delta_B) \quad (9)$$

$$Q_{Etc} = \left(\frac{X_E + X_B}{X_E X_B} \right) V_{Et}^2 - \frac{V_{Et}V_E}{X_E} \cos(\delta_{Et} - \delta_E) - \frac{V_{Et}V_{Bt}}{X_B} \cos(\delta_{Et} - \delta_{Bt}) + \frac{V_{Et}V_B}{X_B} \cos(\delta_{Et} - \delta_B) \quad (10)$$

$$P_{Bt} = \frac{V_{Bt}V_{Et}}{X_B} \sin(\delta_{Bt} - \delta_{Et}) + \frac{V_{Bt}V_B}{X_B} \sin(\delta_{Bt} - \delta_B) \quad (11)$$

As evident, equations (9), (10) and (11) are nonlinear, thus Newton-Raphson method should be applied. The following Jacobian matrix for such power system is found to be:

$$J = \begin{bmatrix} \frac{\partial P_{Et}}{\partial \delta_E} & \frac{\partial P_{Et}}{\partial V_E} & \frac{\partial P_{Et}}{\partial \delta_B} & \frac{\partial P_{Et}}{\partial \delta_B} \\ \frac{\partial Q_{Et}}{\partial \delta_E} & \frac{\partial Q_{Et}}{\partial V_E} & \frac{\partial Q_{Et}}{\partial \delta_B} & \frac{\partial Q_{Et}}{\partial V_B} \\ \frac{\partial P_{Bt}}{\partial \delta_E} & \frac{\partial P_{Bt}}{\partial V_E} & \frac{\partial P_{Bt}}{\partial \delta_B} & \frac{\partial P_{Bt}}{\partial V_B} \\ \frac{\partial Q_{Bt}}{\partial \delta_E} & \frac{\partial Q_{Bt}}{\partial V_E} & \frac{\partial Q_{Bt}}{\partial \delta_B} & \frac{\partial Q_{Bt}}{\partial V_B} \end{bmatrix} \quad (12)$$

4. Simulation Results

The system in Figure 6 has been modeled and simulated using Matlab Program by adding the UPFC and TCSC between Bus 1 and Bus 3. In this case, an active power (P_2) supplied to the grid by the synchronous machine (2) is selected to be 2.479p.u. and the active power (P_1) is considered as variable power demanded by the load. The other parameters are $V_1=1.018$ p.u., $V_2=1.011$ p.u., and the impedance of the reactance of the transmission lines are selected to be: $X_1=0.04$ p.u., $X_2=X_3=0.22$ p.u., and $X_4=0.047$ p.u. [20]. While the load at Bus 3 is assumed to be non-linear load and thus the active power (P_3) and the reactive power (Q_3) can be written as follows [21]:

$$P_3 = P_0 \left(\frac{V}{V_0} \right)^a \quad (13)$$

$$Q_3 = Q_0 \left(\frac{V}{V_0} \right)^b \quad (14)$$

Where; $P_0 = 6.381$ p.u., $Q_0 = 0.2458$ p.u., $V_0=1$ p.u., and a & b are constant values for different types of loads models as presented in Table 2.

For the system shown in Figure 6, the steady state performances of UPFC and TCSC were investigated with regard to the three non-linear load models mentioned in Table 2. For both cases, flow of active power and reactive power at Bus 3 were recorded. In the case of UPFC, active and reactive powers were recorded as the modulation index (M_{pq}) for the series compensation block was varying. On the other hand, active and reactive powers were recorded as the firing angle (α) is varying in the case of TCSC.

Table 2. Typical load model parameters (IEEE, 1993) [21]

Type of load	a	b
Residential	0.9-1.7	2.4-3.3
Commercial	0.5-0.8	2.4-2.5
industrial	0.1-1.8	0.6-2.2

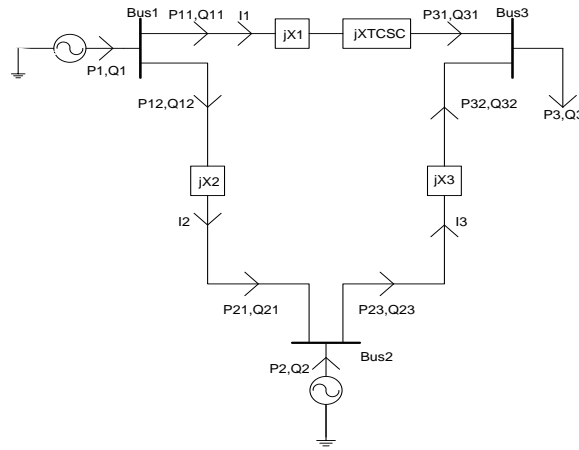


Figure 6. The basic system with adding TCSC

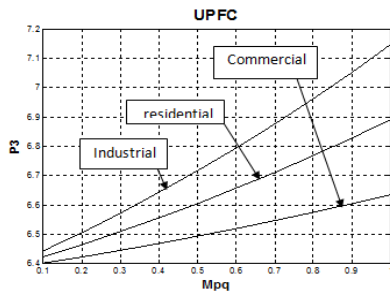


Figure 7. The flow of active power (P_3) at Bus 3 (after adding UPFC to the system) as modulation index is varying and for different types of loads

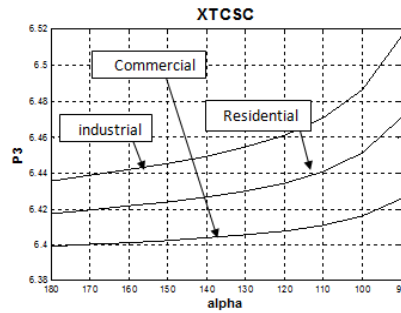


Figure 8. The flow of active power (P_3) at Bus 3 (after adding TCSC to the system) as firing angle (α) is varying and for different types of loads

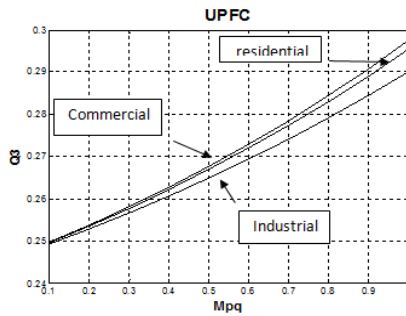


Figure 9. The flow of reactive power (Q_3) at Bus 3 (after adding UPFC to the system) as modulation index is varying and for different types of loads

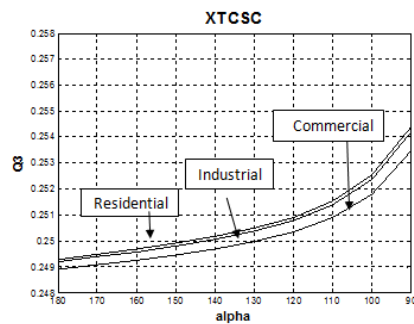


Figure 10. The flow of reactive power (Q_3) at Bus 3 (after adding TCSC to the system) as firing angle (α) is varying and for different types of loads

Figure 7 and 9 represent the flow of active (P_3) and reactive powers (Q_3) at Bus 3 (after adding UPFC to the system) as modulation index is varying and for different types of loads. Conversely, Figure 8 and 10 represent the flow of active (P_3) and reactive powers (Q_3) at Bus 3 (after adding TCSC to the system) as firing angle (α) is varying and for different types of loads. It can be seen that with UPFC more active (P_3) and reactive powers (Q_3) can be

received at Bus 3 for all three types of non-linear load models. In addition, both active (P_3) and reactive powers (Q_3) in case of UPFC are more sensitive in changing the modulation index (M_{pq}). Furthermore, both the active (P_3) and reactive powers (Q_3) are less sensitive to the non-linearity of the load model. However, the active (P_3) and reactive powers (Q_3) in case of TCSC are only sensitive in changing the firing angle (α) when it was between 90° to 110° .

5. Conclusion

The steady-state performances of the UPFC and TCSC as impedance compensation have been modeled. The effectiveness of both FACTS devices were investigated upon installation in multi-machine systems with different non-linear load models. In case of UPFC, a PWM scheme has been used to control the operation of the converters. Regarding TCSC, a firing angle was varied in order to control the operation of the thyristors. In both cases, results demonstrate that active and reactive powers flow distribution in the system transmission lines can be controlled by varying either the modulation index or the firing angle. Comparison simulation results have shown that with installing UPFC more active and reactive powers can be received at the sending end bus for all three types of non-linear load models. In addition, both active and reactive powers are more sensitive in changing the modulation index. Furthermore, both the active and reactive powers are less sensitive to the non-linearity of the load model. However, the active and reactive powers in case of installing TCSC are only sensitive in changing the firing angle (α) when it is between 90° to 110° . Therefore, results from this study clearly encourage the effectiveness of UPFC in comparison to TSCS in terms of increasing power transfer capability applied to non-linear load models.

References

- [1] L Gyugyi. *Unified power flow controller concept for flexible AC transmission systems*. IEE Proceeding-C. 1992; 139(4): 323-331.
- [2] L Gyugyi, NG Hingorani. Advance static VAR compensator using Gate-tran-off thyristors for utility applications. *CIGRE paper*. 1990; 23: 203.
- [3] CR Fuerte-Esquivel, E Acha. *Unified power flow controller: a critical comparison of Newton-Raphson UPFC algorithms in power studies*. IEE Proceeding-C Generation Transmission Distribution. 1997; 144(5).
- [4] L Gyugyi. *Solid-state control of electrical power in an AC transmission system*, International symposium on electric energy converters in power systems. Invited paper T- IP – 4 - (Capri). Italy. 1989.
- [5] HF Wang. *Damping function of unified power flow controller*. IEE Proceeding of Generation, Transmission and Distribution. 1999; 146(1): 81-88.
- [6] EV Larsen, JJ Sanchez-Gasca, JH Chow. Concept for design of FACTS controlling to damp power swings. *IEEE Trans. Power Syst.* 1995; 10(2): 948-956.
- [7] HF Wang. Selection of robust installing locations and feedback signals of FACTS based stabilizers in multi-machine power systems. *IEEE Trans. Power Syst.* 1999; 2: 569-574.
- [8] HF Wang. Modeling multiple FACTS devices into multi-machine power systems and applications. *International Journal of Electrical Power Systems*. 2003; 25(3): 227-237.
- [9] S Ali Al-Mawsawi. Comparing and evaluating the voltage regulation of a UPFC and STATCOM'. *International journal of Electrical power and energy Systems*. 2003; 25(9): 735-740.
- [10] S Ali Al-Mawsawi, MR Qader, KL Lo. Evaluating the voltage regulation of a UPFC using PI and fuzzy logic controller. *COMPEL: The International Journal for Computation and Mathematics in Electrical and Electronic Engineering*. 2002; 21(3): 409-424.
- [11] Salah Kamal El sayed. Comparison of TCSC and UPFC for Increasing Power Transfer Capability and Damping Power System Oscillation. *New York Science Journal*. 2014; 7(9).
- [12] Satyendra Singh, KS Verma. A New Method to Incorporate TCSC in Optimal Power flow Using Genetic Algorithm. *ARNP Journal of Engineering and Applied Sciences*. 2011; 6(7).
- [13] NA kumar, M Rathinakumar, M Yogesh, J Dines. Comparative Study on the Effectiveness of TCSC and UPFC Facts Controllers. *International Journal of Computer Applications*. 2013; 67(5): 975-8887.
- [14] Rakhmad Syafutra Lubis, Sasongko Pramono Hadi, Tumiran. Selection of Suitable Location of the FACTS Devices for Optimal Power Flow. *International Journal of Electrical & Computer Sciences IJECS-IJENS*. 2012; 12(03): 38.
- [15] SH Lee, CC Chu, DH Chang. *Comprehensive upfc models for power flow calculations in practical power systems*. In Power Engineering Society Summer Meeting. 2001; 1: 27-32.

-
- [16] M Noroozian, L Angquist, M Ghandhari, G Andersson. Use of upfc for optimal power flow control. *Power Delivery, IEEE Transactions on*. 1997; 12(4): 1629-1634.
 - [17] R Mohan Mathur, RK Varma. Thyristor-Based FACTS Controllers For Electrical Transmission Systems. A John Wiley & Sons, Interscience Publication. 2002.
 - [18] Nabavi-Niaki, M Iravani. Steady-state and dynamic models of unified power flow controller (UPFC) for power system studies. *IEEE Transactions on Power Systems*. 1996; 11(4): 1937-1943.
 - [19] C Fuerte-Esquivel, E Acha, H Ambriz-Perez. A comprehensive newton-raphson upfc model for the quadratic power flow solution of practical power networks. *IEEE Transactions on Power Systems*. 2000; 15(1): 102-109.
 - [20] WD Stevenson. Elements of power system analysis. Fourth Edition. McGraw-Hill. 1982: 200-202.
 - [21] WW Price, et al. Bibliography on load models for power flow and dynamic performance simulation. *IEEE Transactions on Power Systems*. 1995; 10(1).